

Comment on “Figures of merit for detectors in digital radiography” [Med. Phys. 31, 348–358 and 359–367 (2004)]

Andrew Maidment and Michael Albert

Citation: [Medical Physics 31](#), 2364 (2004); doi: 10.1118/1.1771871

View online: <http://dx.doi.org/10.1118/1.1771871>

View Table of Contents: <http://scitation.aip.org/content/aapm/journal/medphys/31/8?ver=pdfcov>

Published by the [American Association of Physicists in Medicine](#)

Articles you may be interested in

[Erratum: “Contrast-detail analysis of three flat panel detectors for digital radiography” \[Med. Phys.33, 1707–1719 \(2006\)\]](#)

Med. Phys. **33**, 3580 (2006); 10.1118/1.2337636

[Reply to “Comment on ‘Figures of merit for detectors in digital radiography’” \[Med. Phys. 31, 2364–2365 \(2004\)\]](#)

Med. Phys. **31**, 2366 (2004); 10.1118/1.1771891

[Figures of merit for detectors in digital radiography. II. Finite number of secondaries and structured backgrounds](#)

Med. Phys. **31**, 359 (2004); 10.1118/1.1631427

[Figures of merit for detectors in digital radiography. I. Flat background and deterministic blurring](#)

Med. Phys. **31**, 348 (2004); 10.1118/1.1631426

[Signal detectability in digital radiography: Spatial domain figures of merit](#)

Med. Phys. **30**, 2180 (2003); 10.1118/1.1578485

Educational Lectures

Don't miss these fascinating in-booth speakers. Lectures will be held throughout the show during exhibit hours only, in booth #4001.

Joe Ting, PhD

Utilizing EPID for stereotactic cone commissioning and verification in RIT

Sam Hancock, PhD

Isocenter optimization tools for LINAC-based SRS/SBRT

AAPM 2016
Learn and Earn



Users Meeting

Enjoy some delicious dessert while you learn and earn 2 CAMPEP credit hours at our Users Meeting.

Location . . . Marriott Marquis, Washington, DC

Date Sunday, July 31

Time 7-9 PM

**Visit us
at AAPM
Booth #4001**



call or visit
719.590.1077 • radimage.com

© 2016 RadImage Imaging Technology, Inc.
2016-07-06

Letter to the Editor

Comment on “Figures of merit for detectors in digital radiography” [Med. Phys. 31, 348–358 and 359–367 (2004)]

(Received 17 March 2004; accepted for publication 23 May 2004)

[DOI: 10.1118/1.1771871]

To the Editor,

The recent articles by Pineda and Barrett^{1,2} raise many interesting issues regarding the quantitative assessment of imaging systems and the conventional use of Fourier techniques. The authors give examples where the signal-to-noise ratio (SNR) calculated in the conventional manner differs significantly from the exact calculation of the SNR. However, we are concerned that many readers will not appreciate that these examples, while mathematically correct, represent extreme situations unlike any that are likely to be encountered in the clinic or the laboratory.

In particular, in the first article¹ the authors discuss at length a detector which is subject to no source of noise except that inherent in the x-ray fluence. The detector is assumed to demonstrate completely deterministic blurring, characterized by a parameter σ_b . Physically, this would correspond to a detector for which each x ray produces a very large number of secondary quanta that are then spatially distributed in a Gaussian manner before being counted by the detector elements. The authors then consider the SNR for a signal-known-exactly and background-known-exactly (SKE/BKE) task with an object of spatial dimensions σ_s . This task is quite reasonable when σ_s is not significantly smaller than the size of the detector elements. However, the authors then emphasize the analysis of the case where the spatial extent of the signal, σ_s , is only 1% of the size of the one-dimensional detector elements (as per Pineda and Barrett, the detector spacing is used as the unit of length throughout this note) and yet the position of the object is known exactly relative to the detector spacing. We believe that the emphasis on this rather unrealistic situation is likely to mislead many readers.

The key comparisons between the exact calculation of the SNR and the calculations via Fourier techniques are shown by Figs. 5 and 11 (in Appendix B) of the first paper. Figure 5(b) shows that, for objects whose size σ_s is on the same scale as the size of the detector elements, the Fourier calculations track the exact calculations to better than 1%. Figure 5(a) shows that one can obtain a discrepancy if one considers the SKE/BKE detection task with an object of size $\sigma_s = 0.01$ and blurring given by $\sigma_b = 1.0$. This discrepancy is eliminated if the calculation of the noise-power-spectrum (NPS) is performed with a Hann window as in Fig. 11(a). The discrepancy is then on the order of a few percent for the “discrete space Fourier transform” (DSFT) technique, which properly includes the effects of the finite size and spacing of the detector elements, but not the effects of the finite extent of the detector. Figure 11(b) shows, for $\sigma_s = 0.01$, that if the size of the detector is reduced from $M = 256$ to $M = 64$ ele-

ments one again finds a situation where Fourier-based calculations are inaccurate.

To understand these examples better, it is worth considering the matched filters, or masks, that the ideal observer would use for the SKE/BKE detection task. Such a filter instructs the ideal observer on how to produce a decision statistic by combining the measurements of the various detector elements with appropriate weights, where these weights can be positive or negative. Figure 1 of this note shows the matched filter which would be used by the ideal observer assuming a signal of size $\sigma_s = 1$ centered on the 33rd detector element, with $\sigma_b = 1$. In the notation of Pineda and Barrett, this filter corresponds to $\mathbf{K}_g^{-1}\mathbf{g}$ for $M = 64$ and was calculated directly in the spatial domain using LAPACK.³ It is seen that the ideal observer uses the measurement recorded by the 33rd detector element with slight modifications from the data recorded by the immediately adjacent elements.

Figures 2 and 3 of this note show the matched filters used by the ideal observer for $\sigma_b = 1$, $\sigma_s = 0.01$, and $M = 64$, where in Fig. 2 the object is known to be located directly over the center of the 33rd detector element and in Fig. 3 the known position of the object is offset by one-quarter of the spacing of the detector elements. The matched filters now show quite long tails, thus the statistic upon which the ideal observer’s decision depends now requires a delicate cancellation between values of similar magnitude recorded by multiple detector elements. Even if a detector could be sufficiently well characterized so that the calculation of matched filters such as these was meaningful, the task of detecting

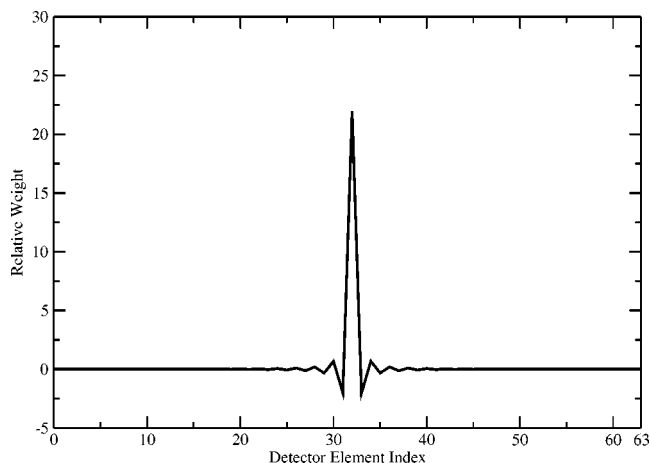


FIG. 1. Matched filter for an object of size comparable to the pixel pitch ($\sigma_s = 1$, $\sigma_b = 1$).

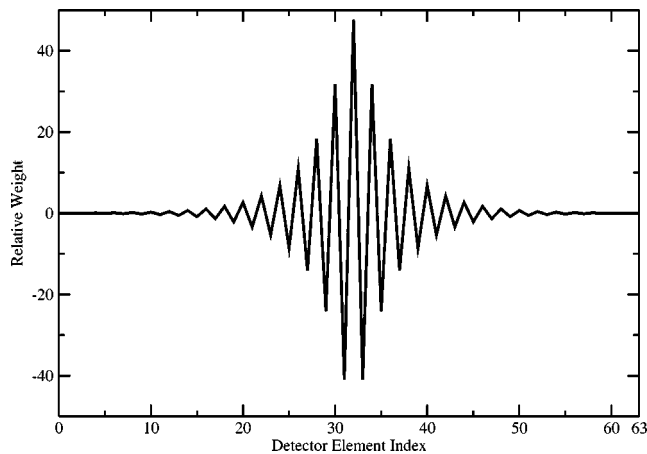


FIG. 2. Matched filter for an object much smaller than the pixel pitch, centered on a pixel ($\sigma_s=0.01$, $\sigma_b=1$).

such a small object whose position was not known *a priori* would presumably require applying about 100 such filters at the position of each detector element. This drastic increase in the number of channels which would need to be monitored would greatly increase the risk of false-positives.

While mathematically correct, it would be truly extraordinary to find a system which is sufficiently free from noise and which is sufficiently well characterized to allow the use of matched filters such as those illustrated here. Indeed, in Fig. 2 of the second paper,² the authors find that the addition of noise due to the production of a reasonable number of secondary quanta (100 per x ray) removes this pathology, and one again finds agreement at the 1% level between the exact calculation and the Fourier technique, particularly when the finite size of the detector elements is taken into account as by the DSFT method.

As a concrete example, the scenario illustrated in Fig. 11(b) of the first paper¹ would be analogous to searching for a 3–4 μm diameter microcalcification using an imaging system with 100 μm detector elements and a total size of 6.4 mm. Extending the detector to just 2.6 cm, or using a detector with typical intrinsic noise sources or imaging a background which is not known exactly would obviate any differences between the exact and Fourier results.

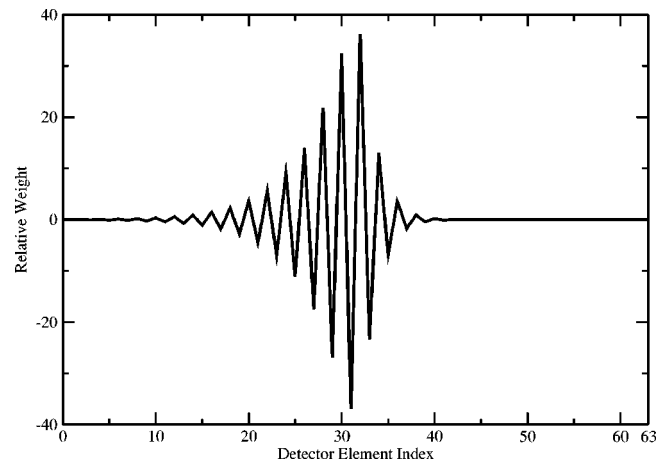


FIG. 3. Matched filter for an object much smaller than the pixel pitch, off-centered by $\frac{1}{4}$ of the pixel ($\sigma_s=0.01$, $\sigma_b=1$).

The continuing introduction of new detector technologies provides a constant impetus for re-evaluating the methods by which detector performance is quantified. Additionally, the number of people looking at quantitative measures is likely to increase. For these reasons we felt it important to clarify the rather unusual nature of the examples given by Pineda and Barrett. Thus, while the exact formulation presented by Pineda and Barrett^{1,2} is robust to issues such as finite detector size, sampling pitch, and aperture width, we feel that, contrary to the authors' conclusions, the cited work supports the use of Fourier techniques for quantifying detector performance in all but the most extreme situations

¹A. R. Pineda and H. H. Barrett, "Figures of merit in digital radiography. I. Flat background and deterministic blurring," *Med. Phys.* **31**, 348–358 (2004).

²A. R. Pineda and H. H. Barrett, "Figures of merit for detectors in digital radiography. II. Finite number of secondaries and structured backgrounds," *Med. Phys.* **31**, 359–367 (2004).

³E. Anderson *et al.*, *LAPACK Users' Guide*, 3rd ed. (SIAM, Philadelphia, 1999).

Andrew Maidment and Michael Albert
 Department of Radiology
 Hospital of the University of Pennsylvania
 Philadelphia, Pennsylvania 19107